Journal of Materials Chemistry C

Accepted Manuscript

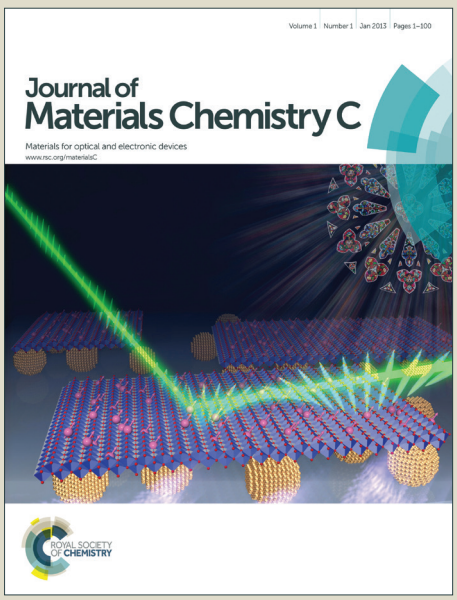

ROYAL SOCIETY OF CHEMISTRY

www.rsc.org/materialsC

Table of Contents

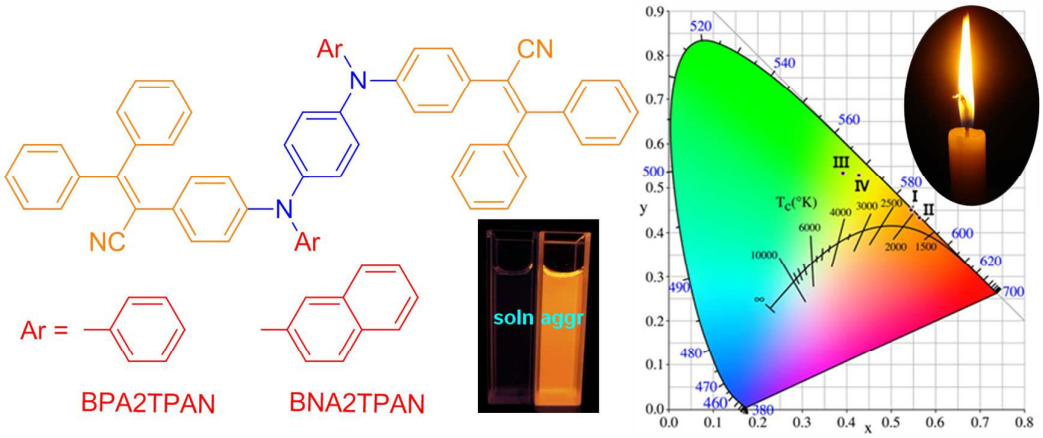

Carefully designed AIE-active luminogens can be utilized to fabricate metal free and nondoped low color temperature OLEDs.

Journal Name

RSCPublishing

ARTICLE

AIE-active, highly thermal and morphological stable, mechanochromic and efficient solid emitters for low color temperature OLEDs

Cite this: DOI: 10.1039/x0xx00000x

Received 00th January 2014,
Accepted 00th January 2014

DOI: 10.1039/x0xx00000x

www.rsc.org/

Yongyang Gong,[a] Jun Liu,[b] Yiren Zhang,[a] Gufeng He,[b] Yang Lu,[a] Wen Bin Fan,[a] Wang Zhang Yuan,*[a] Jing Zhi Sun,[c] and Yongming Zhang*[a]

Low color temperature (CT) lighting sources such as candle light are of significant importance to human health owing to their remarkably less suppression effect on the secretion of melatonin, which helps people relax. As an alternative to hydrocarbon-burning candles, spark and smog free low CT organic light-emitting diodes (OLEDs) are highly desired. So far, however, low CT OLEDs are mainly fabricated by doping technology with several rare-metal complexes and multiple emissive layers. Metal free and nondoped low CT OLEDs remains challenging due to the notorious aggregation-caused quenching (ACQ) effect of traditional chromophores. In this contribution, two luminogens, namely BPA2TPAN and BNA2TPAN, consisting of bisarylamine and two triphenylacrylonitrile (TPAN) units were designed and synthesized. Both luminogens exhibit typical aggregation-induced emission (AIE) characteristics with high solid-state efficiency up to 47.7%. They also possess high thermal stability, outstanding morphological stability as well as obvious mechanochromism. Nondoped OLED devices of the luminogens show physiologically friendly orange light (603, 606 nm) with low CT values of 2093 and 1883 K, which are much lower than those of incandescent bulbs (2000~2500 K) or even candles (~1900 K), whereas their doped OLED devices emit yellow light (551, 559 nm) with significantly improved performance, whose maximal power, current and external quantum efficiencies are 8.3 lm/W, 12.2 cd/A and 4.2%, respectively. These results suggest that AIE luminogens are suitable to fabricate metal-free and nondoped low CT OLEDs with rational molecular design; meanwhile, their electroluminescence can be facilely modulated through doping technology.

Introduction

It is known that color temperature (CT) of light exerts remarkable influence on human physiology and psychology.[1] Bright light with high CT, on the one hand, can stimulate the secretion of cortisol, keeping people awake and active;[1b] on the other hand, greatly suppresses the nocturnal secretion of melatonin, increasing the risk of breast, colorectal and prostate cancers.[1b,1c] Contrastly, low CT light can create romantic atmosphere, and moreover, it shows remarkably less suppressed effect on the secretion of melatonin compared to short-wavelength blue light,[1a] which helps people feel relaxed and therefore beneficial to human health. Due to the drawback of high CT light and the charming property of its low CT counterpart, physicians have long been calling for the development of blue emission free or low CT lighting sources used at night to safeguard human health.[1c]

As a typical low CT light with a long history, candle light is physiologically friendly and romantic at dinner time.[2] However, candle light is generated by burning the hydrocarbon compounds, creating smog, heat and spark with low efficiency (~0.1 lm/W);[2c] moreover it has the risk of causing fire. As an alternative to candles, candle light-style organic light-emitting diodes (OLEDs) are highly desirable. They are inherently energy-saving, smoke- and fire-hazard free, rendering them ideal physiologically friendly lighting devices for use at night or alternative romantic table light for dinner time. Despite the intriguing properties of low CT OLEDs, so far, they are far from being developed. Current electrically-driven lighting devices hardly show CT values smaller than 2000 K, and little attention has been paid to the development of low CT non-white lighting sources. Until recently, low CT OLEDs, particularly candle light-style OLEDs were developed by Jou and co-workers.[2] However, these OLED devices are normally fabricated by several rare-metal complexes with multiple light-emitting layers (LELs). Metal-free and nondoped low CT OLEDs are not reported, which should be mainly ascribed to the notorious aggregation-cause quenching (ACQ) problem[3] of traditional chromophores.

ACQ effect has greatly restricted the practical applications of traditional chromophores because luminescent materials are normally used in aggregated or condensed solid film states. Although intensive efforts have been made to alleviate or eliminate the ACQ effect through chemical or physical methods, such as introduction of bulky alicyclics, encapsulation by

surfactants and blending with transparent polymers,[4] these approaches would inevitably scarify their optoelectronic properties. Fortunately, in 2001, Tang and co-workers discovered a novel phenomenon of aggregation-induced emission (AIE), which is opposite to the ACQ effect.[5] Namely, these compounds are practically nonluminescent in solutions, but become highly emissive in the aggregated states.[5,6] The discovery of AIE phenomenon opens new opportunities for the construction of efficient OLEDs.[7] Generally, even nondoped OLEDs based on AIE-active luminogens also exhibit good performance due to their high solid-state efficiencies.[7-8] Therefore, AIE emitters are promising candidates for low CT OLEDs.

In our recent focus on D-π-A structured efficient solid emitters, it is found that triphenylacrylonitrile (TPAN) exhibits typical crystallization-induced emission (CIE) behaviours, combination of it with other conjugates can readily generate new AIE-active luminogens.[7d,7e,9] D-π-A structures are also effective in tuning the photophysical properties, including emission wavelength and efficiency of the luminogens.[10] Due to the electron withdrawing and CIE features of TPAN, emission properties, particularly solid-state emission colors of the luminogens can be facilely modulated through combination of TPAN with varying electron donating groups such as diphenylamine,[7d] triphenylamine[7e,9] and carbazole.[11] It is thus envisioned that AIE-active D-π-A molecules can be utilized to fabricate nondoped low CT OLEDs through careful molecular design.

In this paper, two D-π-A structured luminogens, namely BPA2TPAN and BNA2TPAN (Chart 1), consisting of two TPAN and bisarylamine units were designed and successfully synthesized. Both compounds are AIE-active, with high solid-state photoluminescence quantum yields (PLQY) of 47.7% and 46.3% for BPA2TPAN and BNA2TPAN, respectively. They show outstanding thermal and morphological stabilities, with degradation temperature (T_d, at which a sample loses its 5% weight)/glass-transition temperature (T_g) being 454/173 and 464/180 ℃, respectively. BPA2TPAN and BNA2TPAN solids also exhibit obvious mechanochromism: upon grinding, the emission maxima of the as prepared powders are changed from 559 and 580 nm to 600 and 605 nm, respectively,. The nondoped OLEDs utilizing both luminogens emit low CT (as low as 1843 K) lights with moderate performance. Meanwhile, their doped counterparts demonstrate distinguished yellow emissions with remarkably enhanced efficiencies.

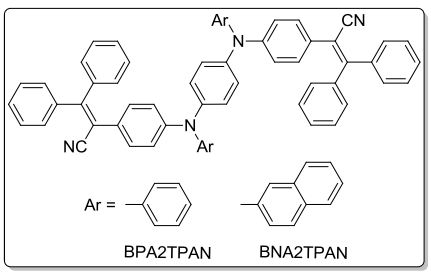

Chart 1 Chemical structure of BPA2TPAN and BNA2TPAN.

Experimental section

Materials. Sodium *tert*-butoxide (*t*-BuONa), sodium hydride (NaH), palladium diacetate [$Pd(OAc)_2$], *N*,*N*′-diphenyl-1,4-phenylenediamine (**2**) and *N*,*N*′-di-2-naphthyl-1,4-phenylenediamine (**3**) were obtained from TCI (Shanghai) Development Co., Ltd. Benzophenone, polystyrene (PS) and 4-bromophenylacetonitrile were obtained from J&K Chemical Scienticfic Ltd. Tri-*tert*-butylphosphine [(t-Bu)$_3$P, 0.5 M in toluene] was purchased from Puyang Huicheng Electronic Material Co., Ltd. Benzene, toluene and dichloroform (DCM) were distilled under normal pressure from calcium hydride (CaH_2) under nitrogen immediately prior to use. Tetrahydrofuran (THF) was distilled from sodium benzophenone ketyl under nitrogen before use. All other commercially available reagents were used as received without further purification.

Instruments. High resolution mass (HRMS) spectra were recorded on a Bruker solariX FTICR mass spectrometer operating in a MALDI mode. Elemental analysis (EA) was recorded on an Elementar Analysensysteme GmbH Vario EL elemental analyzer. Before EA tests, the samples were dried in vacuum at 100 °C overnight. UV-vis absorption and emission measurements were performed on a Perkin-Elmer lambda 35 UV/Vis spectrophotometer and a Perkin-Elmer LS 55 luminescence spectrometer, respectively. PLQYs of the solutions were measured using quinine sulphate as standard ($\Phi_{F,s}$ = 54% in 0.1 N H_2SO_4)[12], while solid-state efficiencies of the as prepared and ground samples were determined using a JASCO FP-6600 fluorescence spectrophotometer equipped with an integrating sphere. The mean diameter (D_m) and polydispersity (PD) of the suspensions for BPA2TPAN and NPA2TPAN in 10/90 THF/water were determined on a Malvern Zetasizer nano ZS90 instrument equipped with a He-Ne laser (λ = 633 nm) at a scattering angle of 90 ° under 25 °C. Thermogravimetric analysis (TGA) and differential scanning calorimetric (DSC) experiments were conducted on a TGA Q5000 V3.13 Build 261 instrument and a Netzsch DSC 200 F3 under nitrogen at the scan rates of 20 and 10 ℃/min, respectively.

Preparation of aggregates for AIE measurement. Stock solutions of the luminogens in THF with a concentration of 100 μM were prepared. An aliquot (1 mL) of the stock solution was transferred to 10 mL volumetric flask. After appropriate amount of THF was added, water was added dropwise under vigorous stirring to furnish 10 μM solution with different fractions of water (0~90 vol%). Photoluminescence (PL) measurement of the resultant samples was performed immediately.

Preparation of the luminogen-doped PS films. 100 mg of PS was added to l ml of THF solution of the luminogen (10 μM). After PS was completely dissolved, the mixture was drop-cast on a glass plate. Then the dried film was peeled off the plate before measurement.

OLED fabrication. The devices were fabricated by the following processes. First, ITO-coated glass substrates were cleaned successively using deionized water, acetone and isopropanol in an ultrasonic bath, and then dried in drying cabinet followed by pretreatment with oxygen plasma. After the organic films of 1,4-bis[(1-naphthylphenyl)-amino] biphenyl (NPB), emission layer, bathophenanthroline (Bphen), and lithium fluoride (LiF) were deposited by the thermal evaporation under a base vacuum of ~10^{-6} torr, aluminium (Al) metal was evaporated in another vacuum chamber without breaking the vacuum. The thicknesses of the films were determined by quartz thickness monitors. The active area of the EL device, defined by the overlap of the ITO and the cathode electrode, was 3 mm × 3 mm. Current density-voltage and current efficiency-current density characteristics were measured with a computer controlled Keithley 2400 Source Meter and

BM-7A Luminance Colorimeter. The electroluminescence (EL) spectra were measured by Labsphere CDS-610. All measurements were carried out under air at room temperature without device encapsulation.

Synthesis of BPA2TPAN. Into a 50 mL two-necked round bottom flask were placed **2** (0.5 mmol, 130 mg), **1** (1.5 mmol, 540 mg), *t*-BuONa (2 mmol, 192 mg), $Pd(OAc)_2$ (0.05 mmol, 11 mg) and $(t\text{-Bu})_3P$ (0.5 mmol, 1 mL). The flask was evacuated under vacuum and flushed with dry nitrogen three times. Then 30 mL of fresh toluene was injected. The mixture was refluxed under stirring for 36 h. Upon cooling to room temperature, it was diluted with 100 mL of chloroform and washed with water and brine. The organic layer was dried over anhydrous magnesium sulfate ($MgSO_4$). After filtration and solvent evaporation, the crude product was purified by silica-gel column chromatography using petroleum ether (PE)/DCM as eluent (4/1~2/1, v/v). The resulting solid was further washed with chloroform/*n*-hexane mixture. A yellow solid was finally obtained in 80% yield. HRMS (MALDI) *m/z*: $[M]^+$ calcd for $C_{60}H_{42}N_4$, 818.3409; found: 818.3376. Anal. calcd for $C_{60}H_{42}N_4$ (%): C 87.99, H 5.17, N 6.84; found: C 88.08, H 5.32, N 6.79.

Synthesis of BNA2TPAN. Compound BNA2TPAN was synthesized according to the similar procedures described above for BPA2TPAN. An orange solid was obtained in 72% yield. HRMS (MALDI) *m/z*: $[M]^+$ calcd for $C_{68}H_{46}N_4$, 918.3722; found 918.3680. Anal. calcd for $C_{68}H_{46}N_4$ (%): C 88.86, H 5.04, N 6.10; found: C 88.83, H 5.25, N 6.29.

Results and discussion

BPA2TPAN and BNA2TPAN were synthesized according to the route shown in Scheme 1. Briefly, **1** was prepared according to the literature method through Knoevenagel condensation reaction between benzophenone and 4-bromophenylacetonitrile.[9,13] Then the target molecules BPA2TPAN and BNA2TPAN were obtained in good yields by Buchwald-Hartwig C–N cross-coupling between **1** and **2** or **3**, utilizing $Pd(OAc)_2$ and $(t\text{-Bu})_3P$ as catalysts under mild conditions.[14] Thin layer chromatography (TLC) examination suggests high purity of the isolated compounds, as only single point is observed for each sample after being developed in 1/1 PE/DCM mixture (Fig. S1, ESI†). However, BPA2TPAN and BNA2TPAN show poor solubility in common organic solvents, it is hence difficult to obtain meaningful ^1H or ^{13}C NMR signals in such deuterated solvents as chloroform-*d*, dimethyl sulfoxide-d_6, acetone-d_6 and THF-d_8. To further identify the final products, HRMS and EA experiments were conducted, with satisfactory results obtained. BPA2TPAN and BNA2TPAN give $[M]^+$ peaks at *m/z* 818.3376 (calcd 818.3409) and 918.3680 (calcd 918.3722) in their HRMS spectra (Fig. S2 and S3, ESI†), confirming the formation of the expected adducts. Moreover, the EA results of C 87.99, H 5.17, N 6.84 and C 88.86, H 5.04, N 6.10 are highly consistent with their theoretical values (BPA2TPAN: C 88.08, H 5.32, N 6.79; BNA2TPAN: C 88.83, H 5.25, N 6.29).

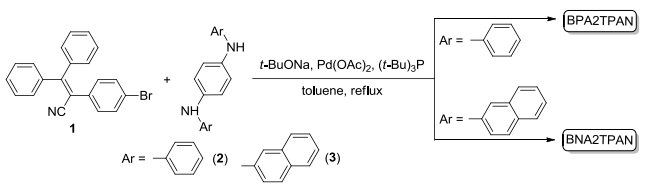

Scheme 1. Synthetic route to BPA2TPAN and BNA2TPAN.

BPA2TPAN shows two absorption peaks at 300 and 399 nm in THF (Fig. 1). While the former is attributable to the π-π* transition, the latter is corresponded to the intramolecular charge transfer (ICT) transition.[15] Similarly, BNA2TPAN depicts two absorption bands at 327 and 394 nm. Compared with BPA2TPAN, the former longer absorption of BNA2TPAN indicates it is more conjugated than BPA2TPAN, whereas the latter slightly shorter band (by 5 nm) suggests naphthyl substituted bisarylamins possesses comparable or even weaker electron donating ability than its phenyl substituted counterpart.

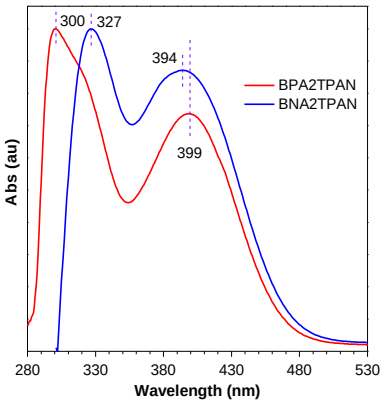

Fig.1 Normalized absorption spectra of BPA2TPAN and BNA2TPAN in THF.

T_d and T_g of organic semiconductors exert great influence on the performance of their optoelectronic devices.[16] Particularly, T_g of the conjugates is one of the most important parameters, which determines the device stability and durability. Therefore, thermal properties of BPA2TPAN and BNA2TPAN were investigated by DSC and TGA. T_g values for BPA2TPAN and BNA2TPAN are as high as 173 and 180 °C (Fig. 2A), respectively, indicating their excellent morphological stability. The higher value of BNA2TPAN should be ascribed to the even more rigid naphthyl units than the phenyl rings. The T_d values of BPA2TPAN and BNA2TPAN reach up to 454 and 464 ℃, respectively; meanwhile, the temperatures for the compounds with 1 wt% weight loss are also as high as 364 and 410 ℃ (Fig. 2B), thus suggesting their wonderful thermal stability. Such outstanding thermal and morphological stabilities render BPA2TPAN and BNA2TPAN highly applicable in optoelectronic devices.[17]

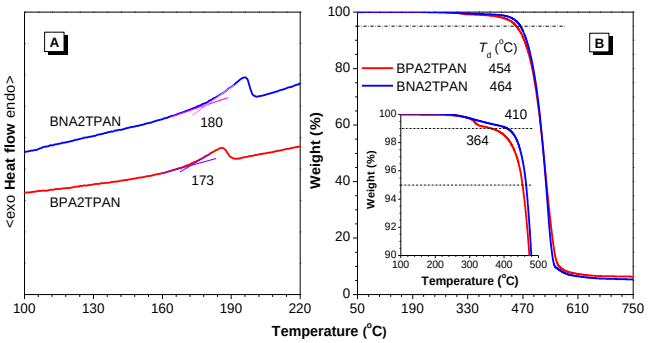

Fig. 2 (A) DSC (second heating cycle) and (B) TGA thermograms of BPA2TPAN and BNA2TPAN recorded under nitrogen at the scan rates of 10 and 20 °C/min, respectively. The inset in (B) is the magnification of partial TGA curves.

TPAN is a typical CIE compound,[9] combination of it with other units as aniline,[18] diphenylamine,[7d] triphenylamine[7e,9] and carbazole[11] yielded new AIE molecules. It is thus envisioned

that BPA2TPAN and BNA2TPAN are also AIE-active. To verify it, PL spectra of BPA2TPAN and BNA2TPAN in THF and THF/water mixtures were measured. Water is chosen because it is a typical nonsolvent for the compounds: the luminogen molecules must aggregate in the THF/water mixtures with high water fractions (f_w). As shown in Fig. 3A and 3B, THF solution of BPA2TPAN does not emit any visible light upon UV irradiation, giving nearly a flat line when emission signal is recorded. With addition of water, the emission remains almost unchanged at $f_w \leqslant 60\%$; However, when f_w reaches 70%, an emission enhancement is observed. Further increasing of f_w gives swiftly increased emission.

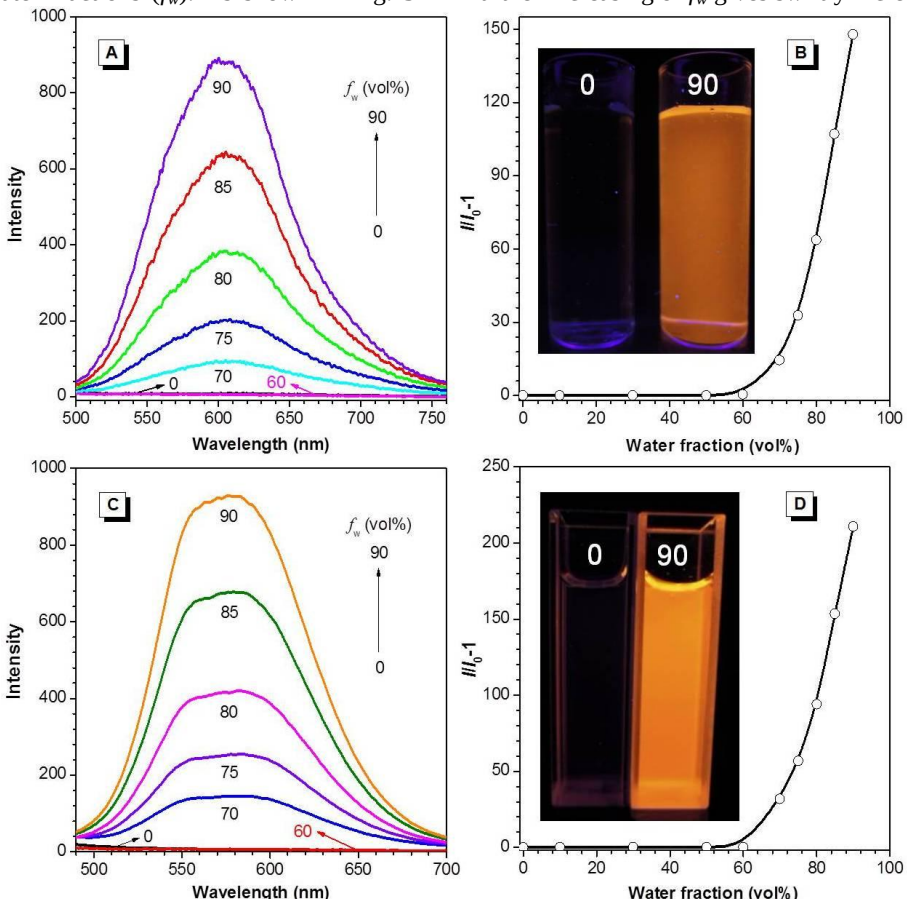

Figure 3. (A, C) PL spectra of (A) BPA2TPAN and (C) BNA2TPAN in THF and THF/water mixtures. (B, D) Plot of PL intensity of (B) BPA2TPAN (606 nm) and (D) BNA2TPAN (582 nm) *vs.* water fractions (f_w). Concentration = 10 μM; excitation wavelength = 400 nm. Insets in (B) and (D) are photographs of BPA2TPAN and BNA2TPAN in THF and 10/90 THF/water mixture taken under UV illumination.

From the molecular solution in THF to the aggregate suspension in 10/90 THF/water mixture (D_m = 155 nm, PD = 0.07, Fig. S4, ESI†), the PL peak intensity of BPA2TPAN at 606 nm is remarkably enhanced by ~148 times, verifying its AIE nature. In THF and low f_w mixtures, BPA2TPAN molecules are still molecularly dissolved. The intramolecular rotations of the molecules are highly active, which effectively consume the exciton energies, thus making the molecules almost nonluminescent. In high f_w mixtures, due to the worsening of the solvating power of the aqueous media, BPA2TPAN molecules start to aggregate, which greatly impedes the intramolecular rotations of the molecules. It renders the excitons deactivated mainly through the radiative path, thus boosting the emission. The inset graph in Fig. 3B also shows the vivid emission contrast of BPA2TPAN in THF and 10/90 THF/water mixture upon UV irradiation.

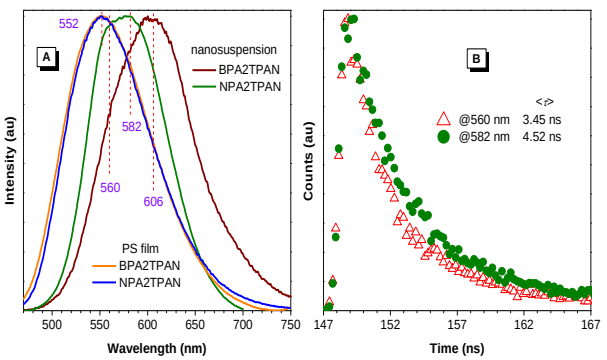

Fig. 4 (A) PL spectra of BPA2TPAN and BNA2TPAN nanosuspensions and doped PS films. (B) PL decay curves of BNA2TPAN nanosuspensions monitored at 560 and 582 nm.

BNA2TPAN shows similar AIE behaviors to those of BPA2TPAN (Fig. 3C and 3D), with an emission enhancement of ~211-fold in 10/90 THF/water as compared to that in THF by aggregate formation (D_m = 179 nm, PD = 0.16, Fig. S5,

ESI†). Notably, while BPA2TPAN aggregates show a single peak at ~606 nm, BNA2TPAN suspensions exhibit broad emissions, which can be further divided into two peaks at 560 and 582 nm, with lifetime (τ) values of 3.45 and 4.52 ns (Fig. 4), respectively. Different τ values suggest the presence of varying emission species. It is assumed that the former and latter peaks are ascribed to the monomer and excimer emissions, respectively. These results indicate that despite only small structure difference between BPA2TPAN and BNA2TPAN, their molecular stacking mode is considerably different in the nanoaggregates. However, when embedded in PS films, they demonstrate almost identical emission profile with the same peak at 552 nm, which is approaching to that of the short-wavelength emission of BNA2TPAN nanoaggregates (560 nm). For BPA2TPAN, the remarkable emission difference between the nanoaggregates (606 nm) and isolated molecules in PS film (552 nm) strongly indicate the former is arisen from the excimers.[19]

To quantitatively evaluate the AIE effect, PLQYs of the luminogens in both solution and as prepared solid states were determined. The $\Phi_{F,s}$ values of BPA2TPAN and BNA2TPAN in THF are as low as 0.09±0.01% and 0.12±0.04% (Table S1, ESI†), thus confirming their practically nonluminescent nature in solvents. However, those of their as prepared solids are boosted to 47.7% (BPA2TPAN) and 46.3% (BNA2TPAN), giving the AIE factors ($\alpha_{AIE} = \Phi_{f,asp}/\Phi_{F,s}$) of 530 and 386, respectively, which are among the highest values for AIE luminogens.[20]

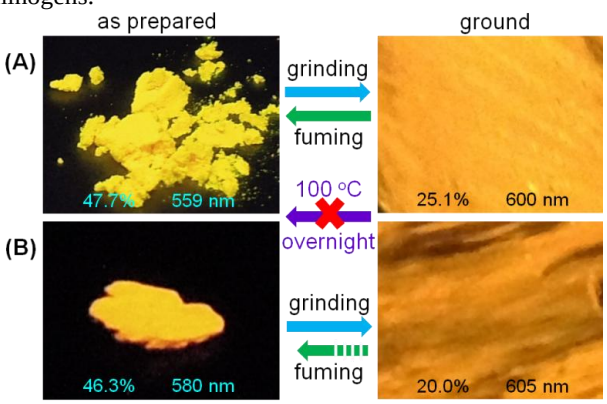

Fig. 5 Photographs of the as prepared solids (left) and ground powders (right) of (A) BPA2TPAN and (B) BNA2TPAN taken under 365-nm UV light irradiation. The quantum efficiency and emission maximum of each sample are as indicated.

High PL efficiency of the as prepared solids and highly twisted conformation of BPA2TPAN and BNA2TPAN make them potentially mechanochromic materials, which are attracting increasing attentions owing to their fundamental importance and potential applications in stress sensor, camouflaging, optical information storage, memory chips, security inks, etc.[21] Upon grinding in an agate mortar with a pestle, the emission color of the as prepared BPA2TPAN changes from yellow to orange (Fig. 5A), with red shifted emission maximum from 559 to 600 nm and increased full width at half maximum (FWHM) from 80 to 109 nm (Fig. 6A). BNA2TPAN behaves similarly to BPA2TPAN, whose emission color varies from yellowish orange to orange (Fig. 5B), accompanying with the changes of emission peak/FWHM from 580/90 to 605/107 nm (Fig. 6B).

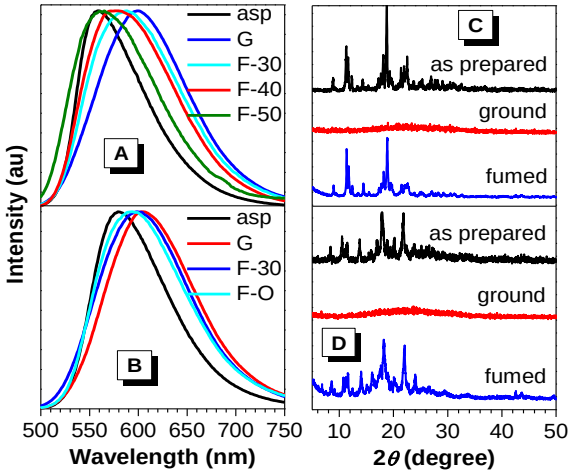

Fig. 6 (A, B) PL spectra and (C, D) XRD patterns of the as prepared solids and ground powders of (A, C) BPA2TPAN and (B, D) BNA2TPAN. Excitation wavelength = 400 nm. Abbreviations: asp = as prepared; G = ground; F-*n* (*n* = 30, 50) = fumed with THF for *n* min; F-O = fumed with THF overnight.

Normally, emission of the ground low T_g luminogens can be easily recovered through heating or fuming treatment.[21] For the ground solids of BPA2TPAN and BNA2TPAN, however, no apparent emission change is detected even when they are annealed at 100 ℃ overnight, indicating their stable conformations owing to the high T_g. Such stable conformation and emission are highly desirable for optoelectronic applications. On the other hand, while the solid emission can generally be fully restored upon solvent fuming for a few minutes or even several seconds, only moderate recovery from 600 to 587 nm (FWHM = 112 nm) is observed for BPA2TPAN even being fumed in THF atmosphere for 30 min. With more fumigation time of 40 and 60 min, its emission maximum gradually recovers to 575 and 563 nm, but still with much broader FWHM of 110 and 103 nm (Fig. 6A). Even more difficult restoration is found for BNA2TPAN. After being fumigated for 30 min, its emission is blue shifted by merely 7 nm (from 605 to 598 nm); Moreover, only partial recovery (592 nm, FWHM = 108 nm) is attained even with overnight treatment (Fig. 6B). These results further verify the excellent morphological stability of the amorphous luminogens.

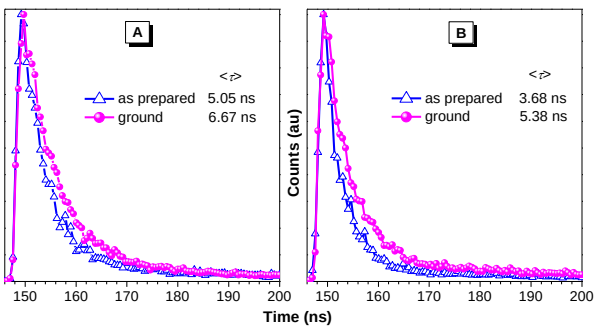

Fig. 7 Time-resolved emission decay curves of the as prepared and ground solids of (A) BPA2TPAN and (B) BNA2TPAN.

To get more insights into the mechanism, XRD measurement of the solids before and after grinding was performed. As shown in Fig. 6C and 6D, the as prepared BPA2TPAN and BNA2TPAN exhibit sharp and intense diffraction peaks, which indicate their well-defined microcrystalline lattices. However, their ground powders do not show any noticeable reflections but with broad diffusion halos in low intensity, suggesting their disordered amorphous nature. Upon fuming in THF atmosphere, sharp peaks coincided with those in the as prepared solids emerge again, revealing the recovery of the ordered crystalline lattice. Clearly, the transition between the ordered crystalline state and disordered amorphous state is crucial to the mechanochromism.

Besides the change of emission color, PL efficiency of the solids after grinding also decreases considerably. Those of ground BPA2TPAN and BNA2TPAN are decreased to 25.1% and 20.0%, respectively, which might be ascribed to the destruction of intermolecular interactions of the solids[7f] as well as the formation of excimers. Normally, decreased emission efficiency would result in shortened lifetime,[22] whereas excimer formation would promote it.[19] Herein, the τ values of the as prepared/ground solids of BPA2TPAN and BNA2TPAN are determined as 5.05/6.67 and 3.68/5.38 ns (Fig. 7), respectively. Decreased efficiency along with increased lifetime of the ground samples verifies the formation of excimers upon mechanical stimuli. Such excimer emissions are highly similar to candle light, whose CT values are calculated as 2131 (BPA2TPAN) and 1843 K (BNA2TPAN) (Fig. S6 ESI†).

Efficient low CT emission at the condensed amorphous state, excellent thermal and morphological stabilities of the luminogens promoted us to explore their potential application in low CT OLED devices. We fabricated multilayer nondoped OLEDs with a general device configuration of ITO/NPB (50 nm)/X (20 nm)/Bphen (40 nm)/LiF (1 nm)/Al (100 nm), where X is BPA2TPAN (device I) or BNA2TPAN (device II), which is used as electroluminescent layer, NPB and Bphen are chosen as hole- and electron-transporting layers, respectively. The EL spectrum, current density-voltage-luminance characteristics, current efficiency, power efficiency and external quantum efficiency of the devices are shown in Fig 8 and summarized in Table 1. Both devices emit orange light with EL maxima (λ_{EL}) at 603 (I) and 606 nm (II), which are rather close to the PL emissions of their ground powders (600 and 605 nm). Devices I and II depict rather low CT values of 2093 and 1883 K, (Fig. 9), which are comparable and even lower than that of candle light (~1900 K).[2d] The device performance is moderate, with maximal luminance (L_{max}), current efficiency (CE_{max}), power efficiency (PE_{max}) and external quantum efficiency (EQE) being 2697 cd/m^2, 2.7 cd/A, 1.9 lm/W, 1.4 % and 2947 cd/m^2, 2.2 cd/A, 1.5 lm/W, 1.3% for devices I and II, respectively. These results clearly imply that properly designed AIE luminogens are quite suitable for the fabrication of metal-free and nondoped low CT OLEDs.

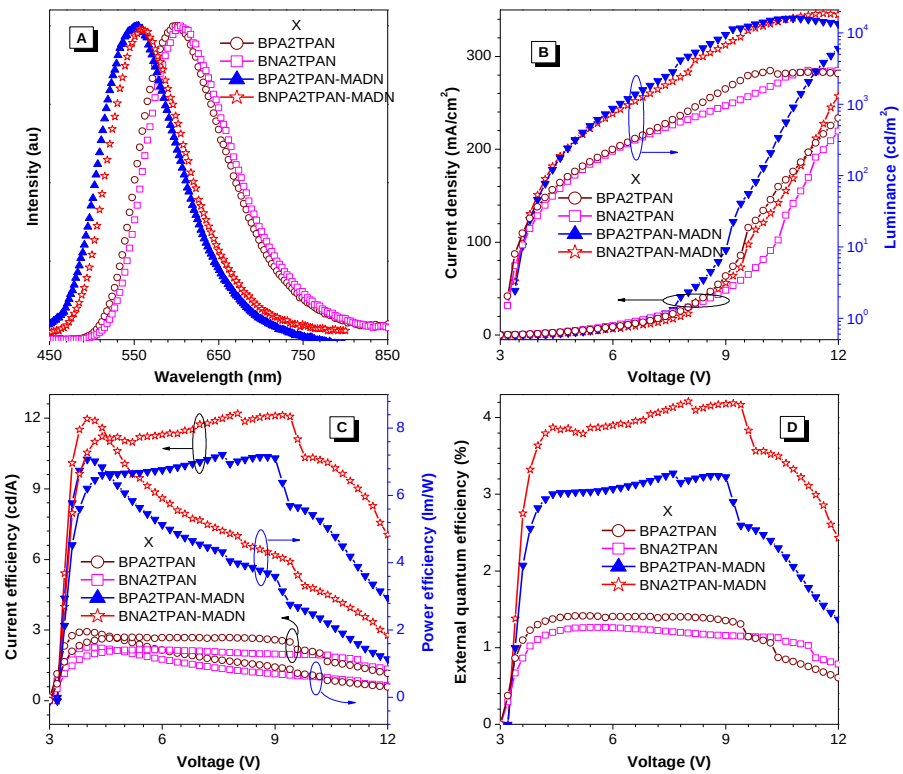

Fig. 8 (A) EL spectra of BPA2TPAN and BNA2TPAN and plots of (B) current efficiency–voltage–luminance, (C) current efficiency, power efficiency, and (D) external quantum efficiency *vs.* driving voltage of the devices with a general configuration of ITO /NPB/X/Bphen/LiF/Al.

Journal Name RSCPublishing

ARTICLE

Table 1. OLED device performances of BPA2TPAN and BNA2TPAN [a]

device	λ_{EL} nm	L_{max} cd/m^2	PE_{max} lm/W	CE_{max} cd/A	*EQE* %	*CT* K
I	603	2697	1.9	2.7	1.4	2093
II	606	2947	1.5	2.2	1.3	1883
III	551	16120	7.1	10.5	3.3	4433
IV	559	18820	8.3	12.2	4.2	3874

[a] Device configuration: ITO/NPB (50 nm)/X (20 nm)/Bphen (40 nm)/LiF (1 nm)/Al (100 nm); X = BPA2TPAN (device I), BNA2TPAN (device II), BPA2TPAN (3%)-MADN (device III), BNA2TPAN (3%)-MADN (device IV); abbreviations: λ_{EL} = EL peak, L_{max} = maximal luminance, PE_{max} = maximal power efficiency, CE_{max} = maximal current efficiency, *EQE* = maximal quantum efficiency.

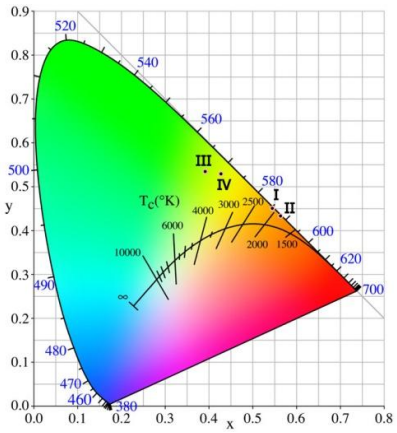

Fig. 9 CIE coordinates and color temperature of the OLED devices of BPA2TPAN and BNA2TPAN.

Nondoped devices of BPA2TPAN and BNA2TPAN emit low CT candle-style lights, which are similar to those of their condensed amorphous solids, but far from those of their molecularly dispersed species embedded in PS (552 nm). It is thus expected that λ_{EL} of the OLEDs can be modulated through simple doping process. Indeed, when BPA2TPAN and BNA2TPAN are doped into 2-methyl-9,10-di(2-naphthyl) anthracene (MADN) at a doping level of 3%, the λ_{EL} values of the resulting devices III and IV are significantly blue shifted to 551 and 559 nm, which are rather close to those of the PS films. Moreover, unprecedentedly, the device performance is dramatically improved by several times. While device IV shows the best performance, with L_{max}, CE_{max}, PE_{max} and *EQE* being 18820 cd/m^2, 12.2 cd/A, 8.3 lm/W and 4.2% (Fig. 8 and Table 1), respectively, those of device III are 16120 cd/m^2, 10.5 cd/A, 7.1 lm/W, and 3.3%. Such considerably enhanced EL performance for the doped devices should be ascribed to the better matching of the energy gaps of each layer and thus more effective charge balance in the devices. These results also suggest the feasibility to regulate the EL color and to promote the device performance based on suchlike AIE luminogens.

Conclusions

In summary, two novel D-π-A structured luminogens, BPA2TPAN and BNA2TPAN, with AIE characteristics and high solid-state efficiency up to 47.7% are synthesized. Both luminogens show high thermal and morphological stabilities, with T_d/T_g values being 454/173 and 464/180 ℃, respectively. They are also mechanochromic: the as prepared crystalline solids of BPA2TPAN and BNA2TPAN emit yellow to orange light with maxima at 559 and 580 nm, whereas their ground amorphous powders fluoresce at 600 and 605 nm with low CT values of 2131 and 1843 K, respectively. Nondoped OLED devices of the luminogens give low CT candle light-style EL with moderate efficiencies. For example, BNA2TPAN based device generates orange EL (606 nm) with L_{max}, CE_{max}, PE_{max} and *EQE* of 2947 cd/m^2, 2.2 cd/A, 1.5 lm/W and 1.3%, respectively. Moreover, CT value of the device is as low as 1883 K, which is even lower than that of candle light (~1900 K). Notably, the doped OLEDs emit significantly blue shifted yellow emissions (551, 559 nm) with considerably enhanced performance, whose L_{max}, CE_{max}, PE_{max} and *EQE* are up to 18820 cd/m^2, 12.2 cd/A, 8.3 lm/W and 4.2%, respectively. The AIE feature, high solid-state efficiency, mechanochromic fluorescence, excellent thermal and morphological stability, and moreover candle light-style low CT OLED emissions and tunable EL color and efficiency of the luminogens render them highly promising candidates for versatile optoelectronic applications.

Acknowledgements

This work was financially supported by the National Science Foundation of China (21104044), the National Basic Research Program of China (973 Program, 2013CB834704), and the he Ph.D. Programs Foundation of Ministry of Education of China (20110073120040). W.Z.Y. thanks the SMC-Chenxing Young Scholar Program of Shanghai Jiao Tong University.

Notes and references

[a] School of Chemistry and Chemical Engineering, Shanghai Key Lab of Electrical Insulation and Thermal Aging, Shanghai Jiao Tong University, Shanghai 200240, China. Fax: +86-21-54742567; Tel: +86-21-34202613; Email: wzhyuan@sjtu.edu.cn (W.Z.Y), ymzsjtu@gmail.com (Y.Z).

[b] National Engineering Lab for TFT-LCD Materials and Technologies, Department of Electronic Engineering, Shanghai Jiao Tong University, Shanghai 200240, China.

[c] Department of Polymer Science and Engineering, Zhejiang University, Hangzhou 310027, China.

† Electronic Supplementary Information (ESI) available. See DOI: 10.1039/b000000x/

References

1 (a) S. W. Lockley, G. C. Brainard, C. A. Czeisler, *J. Clin. Endocrinol. Metab.*, 2003, ***88***, 4502-4505; (b) P. R. Mills, S. C. Tomkins, L. J. Schlangen, *J. Circadian Rhythms*, 2007, ***5***, 2; (c) S. M. Pauley, *Med. Hypotheses*, 2004, ***63***, 588-596; (d) M. Sato, T. Sakaguchi, T. Morita, *Biol. Rhythm Res.*, 2005, ***36***, 287-292.

2 (a) J.-H. Jou, H.-C. Wang, S.-M. Shen, S.-H. Peng, M.-H. Wu, S.-H. Chen, P.-H. Wu, *J. Mater. Chem.*, 2012, ***22***, 8117-8120; (b) J. H. Jou, C. Y. Hsieh, J. R. Tseng, S. H. Peng, Y. C. Jou, J. H. Hong, S. M. Shen, M. C. Tang, P. C. Chen, C. H. Lin, *Adv. Funct. Mater.*, 2013, ***23***, 2750-2757; (c) J.-H. Jou, M.-C. Tang, P.-C. Chen, Y.-S. Wang, S.-M. Shen, B.-R. Chen, C.-H. Lin, W.-B. Wang, S.-H. Chen, C.-T. Chen, F.-Y. Tsai, C.-W. Wang, C.-C. Chen, C.-C. Wang, *Org. Electron.*, 2012, ***13***, 1349-1355; (d) J.-H. Jou, P.-W. Chen, Y.-L. Chen, Y.-C. Jou, J.-R. Tseng, R.-Z. Wu, C.-Y. Hsieh, Y.-C. Hsieh, P. Joers, S.-H. Chen, Y.-S. Wang, F.-C. Tung, C.-C. Chen, C.-C. Wang, *Org. Electron.*, 2013, ***14***, 47-54.

3 (a) S. W. Thomas, G. D. Joly, T. M. Swager, *Chem. Rev.*, 2007, ***107***, 1339-1386; (b) P.-I. Shih, C.-L. Chiang, A. K. Dixit, C.-K. Chen, M.-C. Yuan, R.-Y. Lee, C.-T. Chen, E. W.-G. Diau, C.-F. Shu, *Org. Lett.* , 2006, ***8***, 2799-2802; (c) J. B. Birks *Photophysics of Aromatic Molecules*; Wiley-Interscience, 1970.

4 (a) J.-S. Yang, J.-L. Yan, *Chem. Commun.*, 2008, 1501-1512; (b) S. F. Lim, R. H. Friend, I. D. Rees, J. Li, Y. Ma, K. Robinson, A. B. Holmes, E. Hennebicq, D. Beljonne, F. Cacialli, *Adv. Funct. Mater.*, 2005, ***15***, 981-988; (c) B. S. Gaylord, S. Wang, A. J. Heeger, G. C. Bazan, *J. Am. Chem. Soc.*, 2001, ***123***, 6417-6418.

5 (a) J. Luo, Z. Xie, J. W. Y. Lam, L. Cheng, H. Chen, C. Qiu, H. S. Kwok, X. Zhan, Y. Liu, D. Zhu, B. Z. Tang, *Chem. Commun.*, 2001, 1740-1741; (b) Y. Hong, J. W. Y. Lam, B. Z. Tang, *Chem. Soc. Rev.*, 2011, ***40***, 5361-5388.

6 (a) B.-K. An, S.-K. Kwon, S.-D. Jung, S. Y. Park, *J. Am. Chem. Soc.*, 2002, ***124***, 14410-14415; (b) YY. Gong, YQ. Tan, J. Mei, YR. Zhang, WZ. Yuan, YM. Zhang, JZ. Sun, B. Z. Tang, *Sci. China Chem*., 2013, ***56***, 1178-1182; (c) YY. Gong, YQ. Tan, H. Li, YR. Zhang, WZ. Yuan, YM. Zhang, JZ. Sun, B. Z. Tang, *Sci. China Chem*., 2013, ***56***, 1183-1186; (d) J. Shi, N. Chang, C. Li, J. Mei, C. Deng, X. Luo, Z. Liu, Z. Bo, Y. Q. Dong, B. Z. Tang, *Chem. Commun.*, 2012, ***48***, 10675-10677.

7 (a) W. Z. Yuan, P. Lu, S. Chen, J. W. Y. Lam, Z. Wang, Y. Liu, H. S. Kwok, Y. Ma, B. Z. Tang, *Adv. Mater.*, 2010, ***22***, 2159-2163; (b) Z. Chang, Y. Jiang, B. He, J. Chen, Z. Yang, P. Lu, H. S. Kwok, Z. Zhao, H. Qiu, B. Z. Tang, *Chem. Commun.*, 2013, ***49***, 594-596; (c) J. Huang, N. Sun, Y. Dong, R. Tang, P. Lu, P. Cai, Q. Li, D. Ma, J. Qin, Z. Li, *Adv. Funct. Mater.*, 2013, ***23***, 2329-2337; (d) Y. Gong, Y. Tan, J. Liu, P. Lu, C. Feng, W. Z. Yuan, Y. Lu, J. Z. Sun, G. He, Y. Zhang, *Chem. Commun.*, 2013, ***49***, 4009-4011; (e) W. Z. Yuan, Y. Tan, Y. Gong, P. Lu, J. W. Y. Lam, X. Y. Shen, C. Feng, H. H. Y. Sung, Y. Lu, I. D. Williams, J. Z. Sun, Y. Zhang, B. Z. Tang, *Adv. Mater.*, 2013, ***25***, 2837-2843.

8 (a) Z. Guo, W. Zhu, H. Tian, *Chem. Commun.*, 2012, ***48***, 6073-6084; (b) S. Chen, Z. Zhao, B. Z. Tang, H. S. Kwok, *J. Phys. D: Appl. Phys.*, 2010, ***43***, 095101; (c) P. I. Shih, C. Y. Chuang, C. H. Chien, E. W. G. Diau, C. F. Shu, *Adv. Funct. Mater.*, 2007, ***17***, 3141-3146; (d) H.-C. Yeh, S.-J. Yeh, C.-T. Chen, *Chem. Commun*., 2003, 2632-2633.

9 W. Z. Yuan, Y. Gong, S. Chen, X. Y. Shen, J. W. Y. Lam, P. Lu, Y. Lu, Z. Wang, R. Hu, N. Xie, H. S. Kwok, Y. Zhang, J. Z. Sun, B. Z. Tang, *Chem. Mater.*, 2012, ***24***, 1518-1528.

10 (a) B. Wang, Y. Wang, J. Hua, Y. Jiang, J. Huang, S. Qian, H. Tian, *Chem. Eur. J.*, 2011, ***17***, 2647-2655; (b) Z. R. Grabowski, K. Rotkiewicz, W. Rettig, *Chem. Rev.*, 2003, ***103***, 3899-4032; (c) J. Cremer, P. Bauerle, *J. Mater. Chem.*, 2006, ***16***, 874-884; (d) X. Zhang, J. W. Shim, S. P. Tiwari, Q. Zhang, J. E. Norton, P.-T. Wu, S. Barlow, S. A. Jenekhe, B. Kippelen, J.-L. Bredas, S. R. Marder, *J. Mater. Chem.*, 2011, ***21***, 4971-4982; (e) L. Yao, S. Zhang, R. Wang, W. Li, F. Shen, B. Yang, Y. Ma, *Angew. Chem.*, 2014, ***126***, 2151-2155.

11 Y. Lu, Y. Tan, Y. Gong, H. Li, W. Yuan, Y. Zhang, B. Tang, *Chin. Sci. Bull.*, 2013, ***58***, 2719-2722.

12 W. H. Melhuish, *J. Phys. Chem.*, 1961, ***65***, 229-235.

13 S. Wang, W. J. Oldham, R. A. Hudack, G. C. Bazan, *J. Am. Chem. Soc.*, 2000, ***122***, 5695-5709.

14 T. Yamamoto, M. Nishiyama, Y. Koie, *Tetrahedron Lett.*, 1998, ***39***, 2367-2370.

15 J. M. Hancock, A. P. Gifford, Y. Zhu, Y. Lou, S. A. Jenekhe, *Chem. Mater.*, 2006, ***18***, 4924-4932.

16 (a) K. Naito, A. Miura, *J. Phys. Chem.*, 1993, ***97***, 6240-6248; (b) C.-W. Ko, Y.-T. Tao, *Synth. Met.*, 2002, ***126***, 37-41; (c) Y.-C. Tsai, J.-H. Jou, *Appl. Phys. Lett.*, 2006, ***89***, 243521-243523.

17 Q.-X. Tong, S.-L. Lai, M.-Y. Chan, K.-H. Lai, J.-X. Tang, H.-L. Kwong, C.-S. Lee, S.-T. Lee, *Chem. Mater.*, 2007, ***19***, 5851-5855.

18 Y. Gong, Y. Zhang, W. Z. Yuan, J. Z. Sun, Y. Zhang, *J. Phys. Chem. C*, 2014, ***118***, 10998-11005.

19 (a) T. Seko, K. Ogura, Y. Kawakami, H. Sugino, H. Toyotama, J. Tanaka, *Chem. Phys. Lett.*, 1998, ***291***, 438-444; (b) M. Jaseer, E. Prasad, *J. Photochem. Photobiol., A* 2010, ***214***, 248-256.

20 (a) W. Z. Yuan, S. Chen, J. W. Y. Lam, C. Deng, P. Lu, H. H. Y. Sung, I. D. Williams, H. S. Kwok, Y. Zhang, B. Z. Tang, *Chem. Commun.*, 2011, ***47***, 11216-11218; (b) Z. Zhao, S. Chen, X. Shen, F. Mahtab, Y. Yu, P. Lu, J. W. Y. Lam, H. S. Kwok, B. Z. Tang, *Chem. Commun.*, 2010, ***46***, 686-688.

21 (a) Y. Sagara, T. Kato, *Nat. Chem.*, 2009, ***1***, 605-610; (b) A. Pucci, G. Ruggeri, *J. Mater. Chem.*, 2011, ***21***, 8282-8291; (b) A. Pucci, R. Bizzarri, G. Ruggeri, *Soft Matter*, 2011, ***7***, 3689-3700; (c) Z. Chi, X. Zhang, B. Xu, X. Zhou, C. Ma, Y. Zhang, S. Liu, J. Xu, *Chem. Soc. Rev.*, 2012, ***41***, 3878-3896; (d) C. Weder, *J. Mater. Chem.*, 2011, ***21***, 8235-8236; (e) M.-J. Teng, X.-R. Jia, S. Yang, X.-F. Chen, Y. Wei, *Adv. Mater.*, 2012, ***24***, 1255-1261; (f) C. Dou, D. Chen, J. Iqbal, Y. Yuan, H. Zhang, Y. Wang, *Langmuir*, 2011, ***27***, 6323-6329; (g) X. Luo, J. Li, C. Li, L. Heng, Y. Q. Dong, Z. Liu, Z. Bo, B. Z. Tang, *Adv. Mater.*, 2011, ***23***, 3261-3265; (h) X. Luo, W. Zhao, J. Shi, C. Li, Z. Liu, Z. Bo, Y. Q. Dong, B. Z. Tang, *J. Phys. Chem. C*, 2012, ***116***, 21967-21972.

22 Y. Ren, J. W. Y. Lam, Y. Dong, B. Z. Tang, K. S. Wong, *J. Phys. Chem. B*, 2005, ***109***, 1135-1140.

